# Graph-like state of matter: 12. Static and dynamic entanglements*

**M. Gordon and K. R. Roberts**
*Institute of Polymer Science, University of Essex, Wivenhoe Park, Colchester CO4 3SQ, UK*
*(Received 26 January 1979)*

It is shown that the contribution of chain entanglements to the *equilibrium* shear modulus, recently deduced theoretically and measured experimentally, cancel almost quantitatively the downward adjustment in the front-factor $g$ of the equation of state used in such theories. This downward revision of $g$ is contested theoretically on algebraic grounds, and the classical value of unity is recovered as a result. This classical value is supported by reinterpreting literature data on silicone rubbers by Valles and Macosko, and by new measurements (which confirm less accurate ones obtained earlier by a more difficult method) on a well-tried polyester system near its gel point. There are indications that the contributions of entanglements to the equilibrium shear modulus are all too easily overestimated by theory, and the technologist is advised to prefer the remarkably simple formulae of the graph-like-state theory of phantom chains. Dynamic entanglements can readily explain qualitatively the anelastic effects here reported, viz. frequency shifts in the plot of the real part of the *dynamic* shear modulus against conversion in the range $\alpha/\alpha_c \leqslant 1.01$ (where $\alpha_c$ is the critical conversion at the gel point). Here too it seems as if graph-like-state theory will ultimately account for the observations, but at least certain eigenvalue problems will have to be solved first. An intriguing observation, that at the gel point of the polyester system the spectrum of relaxation frequencies approaches a block distribution, so that every finite value is equally likely, may have general validity.

## INTRODUCTION

On re-examining the classical network theory of rubber elasticity some investigators[1,2] have tried to prove that it 'overrates the restriction of freedom caused by a crosslink' and to correct it accordingly. However, as we shall document, recent searching experimental studies fail to detect such overrating, since measured moduli are not significantly below those calculated by the classical formulae. Accordingly, agreement with experiment of the 'corrected' network theory has required a further compensating correction which happens to restore the equilibrium modulus essentially to its former magnitude. This compensating correction has been based – not on the intrinsic (one-dimensional) theory of network graphs – but on the celebrated effects of entanglements which are supposed to arise from embedding the network graph in a three-dimensional space. By adjustment of an empirical constant concerning these effects, satisfactory agreement with experiment seems to be restored. We shall present our objections to the two compensating corrections, and conclude that, imperfect though the classical theory might be when compared to much more exact experiments than are possible at present, the technologist would be ill-advised to attempt corrections at this stage.

## THEORY OF THE FRONT FACTOR

Duiser and Staverman[1] argued the need for their correction of the network theory very strongly, claiming that the classical formula for the configurational free energy (in the usual notation):

$$\Delta F_c = kT\frac{\nu}{2}\frac{\overline{r^2}}{\overline{r_0^2}}[\alpha_x^2 + \alpha_y^2 + \alpha_z^2 - 3] \qquad (1)$$

was untenable, and should be changed to

$$\Delta F_c = kT\left[\frac{f-2}{f}\right]\frac{\nu}{2}\frac{\overline{r^2}}{\overline{r_0^2}}[\alpha_x^2 + \alpha_y^2 + \alpha_z^2 - 3] \qquad (2)$$

Graessley[2] obtained the same correction with a more transparent form of the averaging procedure employed. His argument is elegant and seems persuasive; we therefore detail our objection to it.

*Figure 1* portrays Graessley's tree-like $j$th-order network for $f = 4$ active functionalities and $j = 3$ (where $j$ is the index of the highest generation as shown). The junctions fixed randomly in 3-dimensional space are marked by stars. By integration, he finds:

$$\Delta F_c = R_j(f)\frac{\nu kT}{2}[\alpha_x^2 + \alpha_y^2 + \alpha_z^2 - 3] \qquad (2a)$$

(The multiple integration, as usual in graph-like-state theory, factorizes into identical single integrations, as the solution of an eigenvalue problem whose eigenvalues 'fortunately' cancel from the treatment. The initial embedding in 3-D space is thus reduced to a formality).

In equation (2a), $R_j(f)$ is given (dropping reference to $f$

* Based on a lecture to the International Rubber Conference, Kiev, USSR, October 1978

0032–3861/79/060681–10$02.00

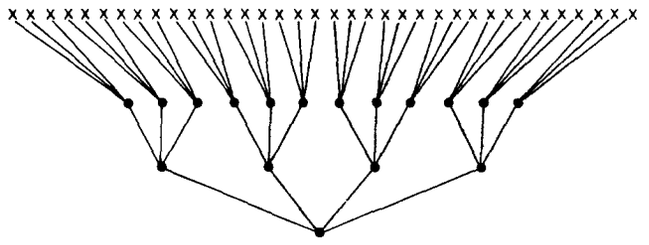

*Figure 1* Graessley's[2] 3rd order network (schematic). The active junction point, shown as the root of the family tree, makes a contribution to the modulus calculated on the assumption that after $j = 3$ generations the junctions (crosses) are *fixed* in random (average) positions. Circles denote *mobile* junctions

throughout) by:

$$R_j \equiv F_j - \frac{1}{N_j} \tag{3}$$

where $F_j$ is the fraction of chains with one fixed end:

$$F_j = (f-2)(f-1)^{j-1}/[(f-1)^j - 1] \tag{4}$$

and $N_j$ the total number of strands:

$$N_j = f[(f-1)^j - 1]/(f-2) \tag{5}$$

Graessley gives an elegant alternative to (3):

$$R_j = \frac{f-1}{f} F_j + \frac{f-2}{f}(1-F_j) \tag{6}$$

in which the coefficients of $F_j$ and $(1-F_j)$ no longer depend on $j$. He therefore feels free to apply equation (6) to more realistic networks than *Figure 1*, i.e. networks with few fixed junctions so that $F_j \to 0$ rather than $F_j \to (f-2)/(f-1)$ as $j \to \infty$ (equation 4). This he achieves by putting $F_j = 0$ in equation (6), to obtain:

$$R_j = (f-2)/f \quad (j = 1,2,\ldots) \tag{7}$$

But is this valid?

Equation (6) follows by algebra from equations (3)–(5). Putting $F_j = 0$ in equation (6) is equivalent to putting $F_j = 0$ in equation (4). Accordingly, for the *given network* (*Figure 1*), $F_j = 0$ is legitimate only for two cases of no physical significance, viz. $f = 1$ and $f = 2$. From equations (3)–(5) we can obtain the solution (when $F_j = 0$):

$$R_j = -(f-2)/f[(f-1)^j - 1] \tag{8}$$

Algebra does not allow the choice of equation (7) as being physically the significant one. Algebra allows no contradiction between equations (7) and (8), and they do agree precisely for those values of $f$, viz. 1 and 2, for which the algebra is legitimate.

The derivation of equation (2a) shows no prospect that, in these circumstances, equation (7) can be applied to arbitrary *different networks*, constructed so that $F_j \to 0$ as $j \to \infty$. The realistic networks exhibit this asymptotic behaviour of $F_j$ not because *fixed* junctions in *Figure 1* should be redefined as *free*, but rather because the fixed junctions are overcounted in *Figure 1* in a specific way. Many of the *distinct* junctions which would be shown for large $j$ are in reality to be *identified* because of cycle formation. In a valuable part of his analysis, Graessley shows that for his networks (*Figure 1*) the effect of cycles on the front-factor $R_j(f)$ in equation (2a) is negligible (see Imai and Gordon[3]) provided small cycles (for $j = 1,2,3$, say) are rare. That they *are* rare arises from the breakdown (over short times involved in crosslinking) of Gaussian statistics of chain conformations in gels, as implied in a forceful statement by James and Guth[4], cited by Gordon, Ward and Whitney[5], (cf. Gordon and Ross-Murphy[6], Dušek *et al.*[7]). It follows from the negligibility of cycles that the appropriate form of $R_1$ is already the correct estimate of the front factor. Now equations (3)–(5) give

$$R_1 = (f-1)/f \tag{9}$$

However, Graessley also presents a calculation for essentially the same kind of network, but now built up around a central strand instead of a central junction. This is a better procedure for calculating $R_1$ and it yields:

$$R_1 = 1 \tag{10}$$

In accepting this as the best estimate for the front factor contribution from the network structure, we thus return exactly to the value originally championed by Wall and Flory[8], which implies a factorization of the partition function into equal contributions from each active network chain.

## CALIBRATION OF CONVERSION IN A NETWORK-FORMING REACTION BY CHEMICAL KINETICS

The testing for proposed correction factors to the classical elasticity theory demands high experimental accuracy. The exploitation of the accuracy of time measurements by calibrating the successive states of cure of a given sample in the framework of chemical kinetics[5] seems almost mandatory. The choice of a single link-forming reaction, not prone to side reactions (a danger with urethane reactions[9]), and whose kinetic mechanism is clearly established in micro- and macromolecular substrates, is highly desirable. Our choice has long settled on self-catalysed esterification, extensively studied by Hinshelwood[10], Flory[11], and many others. In absence of substitution effects[12], and when cyclization is allowed for[13], the bulk reaction is second order in COOH and first order in OH within the small experimental error up to well past the gel point. In benzene 1,3,5-triacetic acid (BTA)/decamethylene glycol (DMG), substitution effects (see Gordon and Leonis[12]) are certainly not measurable and cyclization effects on statistical parameters like the weight-average degree of polymerization $DP_w$ or the number $\nu'_e$ of elastically active network chains (EANCs) per BTA unit are amply corrected by rescaling the gel point from its theoretical value $\alpha_{c,\,\mathrm{theor}} = 0.707$ in absence of cyclization to the measured overall critical converison $\beta_c = 0.724$, which includes a cyclization component. The cyclization component is somewhat smaller than $\beta_c - 0.707$, because cyclization increases slightly the number of intermolecular links needed for gelation[13,14]. For the DMG/BTA system, then, we calculate $\alpha_{\mathrm{theor}}$ by equating $\alpha_{\mathrm{theor}}/\alpha_{c,\,\mathrm{theor}} = \beta/\beta_c$.

*Figure 2* shows one of two similar third-order rate plots for self-catalysed DMG/BTA polyesterification, determined by titration with 0.1 N methanolic NaOH in methyl ethyl ketone/methyl alcohol (50/50 w/w). Very slight concavity upward is expected due to the minute cyclization effect in

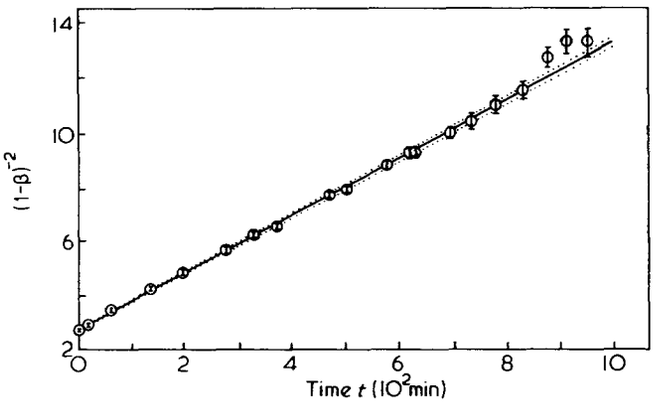


*Figure 2* Third-order rate plot for stoichiometric ($r$ = 1) DMG/BTA, showing error bars for individual points

*Table 1* Kinetic calibration of rate constant and gel points at 90°C for DMG/BTA in the melt

| | Gel time (min) | Rate constant, $k$ ($min^{-1}$) | $\beta_c$ |
|---|---|---|---|
| Run 14 | 935 | 0.00526 ± 0.00006 | 0.721 ± 0.003 |
| Run 15 | 1006 | 0.00522 ± 0.00004 | 0.726 ± 0.003 |

this system. The heavy line is the best-weighted least-square fit to the data (the accuracy decreases with increasing conversion as shown by error bars); the light lines denote confidence limits of 95%. The derived parameters are shown for both runs in *Table 1* together with their standard deviations.

Gel times are not expected to be reproducible, because the reaction at 90°C is started after a variable amount of initial fast reaction at 170°C to promote homogeneous conditions. Each individual gel time was determined by the method of Covas *et al.*[15]. The viscosity is measured as a function of time and assumed to be related to the weight-average molecular weight $\bar{M}_w$ by a Mark–Houwink relation:

$$\log_{10}\eta = K + K'\log_{10}\bar{M}_w \qquad (11)$$

Then $\bar{M}_w$ is calculated as a function of time, by first evaluating $\beta = \beta(t)$ from the rate constant (*Table 1*) and the gel time $t_c$. The typical determination of $t_c$ by least-square linearization of a plot according to equation (11) is shown in *Figure 3* The calculation of $\bar{M}_w$ from $\beta$ follows (with justifiable neglect of cyclization) the formulae derived from cascade theory[15].

Evaluating viscosity measurements over 11 runs with the falling-sphere method and 13 runs by the Weissenberg rheogoniometer, we found the constant $K'$ in equation (11) to be 1.03 with standard deviation $\sigma$ = 0.05. This result agrees with the graph-like-state model ($K'$ = 1.0), or percolation on a Cayley tree, as first formulated for polycondensation by Flory and Stockmayer. The result is quite incompatible with scaling and group-renormalization theory depending on an embedding space[16] ($K'$ = 1.2).

## FITTING OF TWO SETS OF COMPLEMENTARY DATA TO GRAPH-LIKE-STATE THEORY

The data of Valles and Macosko[17] and our present measurements, fitted in this section to the same graph-like-state theory, are complementary in two ways.

(i) The former deal with networks built from primary chains by end-linking, while the latter relate to polyesterification networks built from a polyfunctional micromolecular mixture

(ii) Valles and Macosko deal with relatively high degrees of crosslinking, $G' = 10^4$–$3 \times 10^5$ $Nm^{-2}$, where their silicone rubbers have attained perfect elastic behaviour ($G'' = 0$, their *Figure 1*), while ours cover the range from almost $G' = 0$ to $3 \times 10^3$, and where anelastic effects require extrapolation of $\omega \to 0$ (see *Figures 8–10* below).

Their silicone networks are constructed according to the reactions

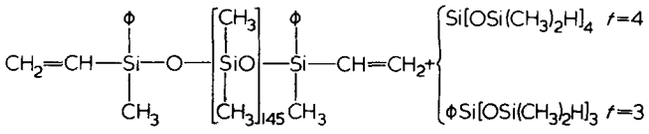


(12)

Their kinetic measurements are fitted to the following equation (their *Figure 2*) with more noticeable systematic deviations than those which emerge from the more sensitive plot of *Figure 2* for polyesterification:

$$d[-SiH]/dt = 1.07 \times 10^{-4}[-SiH]^{2.2} \qquad (13)$$

This equation is, moreover, an empirical one with fractional reaction order, not supported by mechanistic analysis, unlike esterification, which features two *integral* orders. Nevertheless, we regard the data on the silicone reaction as perfectly serviceable.

### *Refitting of data on end-linked silicone rubbers*[17]

We refit the data of Valles and Macosko on:

(a) three-functional branch units ($f$ = 3 in equation 12) and stoichiometric ratio $r$ = 1 (of functionalities of branch-units to funtionalities at primary chain ends). The original data and fittings are shown in their *Figure 5*, and the refitting in our *Figures 4* and *5*;

(b) We also refit the data in their *Figure 3* for $f$ = 4, $r$ = 1 in our *Figure 6*, and

(c) the data in their *Figure 4* for $f$ = 4, $r$ = 1.56 (stoichiometric inbalance) in our *Figure 7*.

Our refittings employ the following equations, which are readily derived from the formalism given by Dobson and Gordon[18] on the (graph-like) notion of Scanlan–Case-type active network chains. Thus we find for $r$ = 1 and any func-

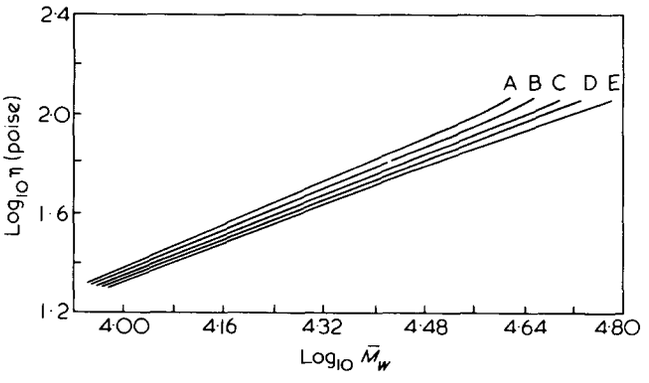


*Figure 3* Viscometric calibration of gel point[15], run 29. Assumed $t_c$: 169.0 min (A), 172.0 (B), 175.0 (C), 178.0 (D), 181.0 (E). Optimal linearity occurs at C ($t_c$ = 175.0 min). Each line contains 102 measured points used in optimization. Their scatter from the lines shown is not noticeable on this scale

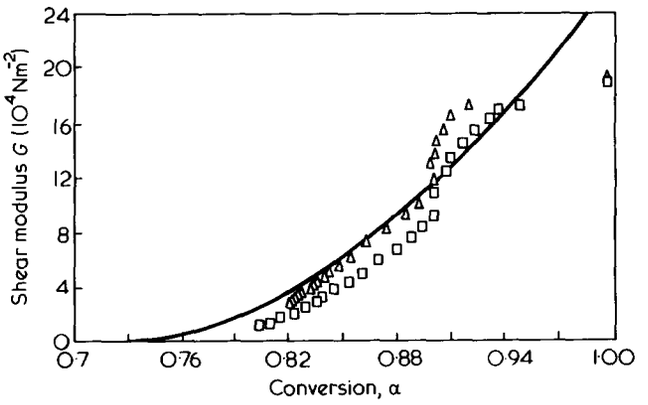


*Figure 4* Valles and Macosco's[17] *Figure 5,* showing shear modulus against extent of reaction in the silicone system ($f = 3$, equation 12). Here refitted to optimize one run (triangles) to equation (18) with $r = 1$. For parameter $g$ see *Table 1*

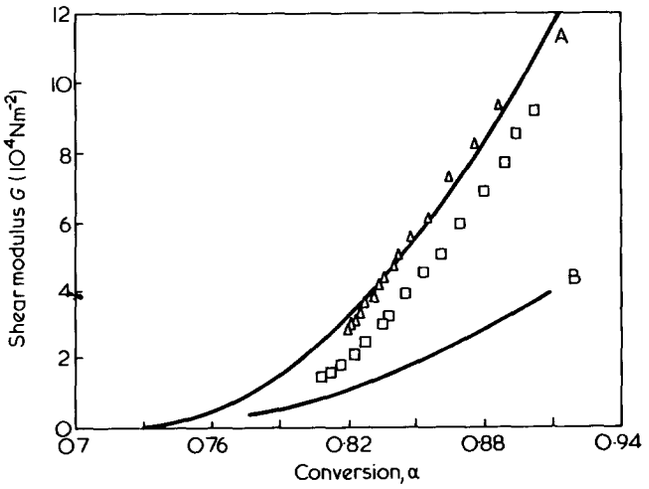


*Figure 5* A, As *Figure 4* but omitting irregular high-modulus results from optimization; B, Plot for $g = 1/3$ in equation (18) or $\epsilon = 0$ (absence of entanglements) in equation (22). Close to the gel point (see *Figures 8–10* for DMG/BTA), the entanglement term in $\epsilon$ becomes negligible and thus allows $g$ to be determined

tionality $f$ of the branch units the number of active network chains per branch unit:

$$\nu'_e = \frac{1}{2}\sum_{i=3}^{f} i\binom{f}{i}(1-\alpha+\alpha\upsilon)^{f-i}(1-\upsilon)^i\alpha^i \qquad (14)$$

where $\nu$ is the extinction probability for a link leading from an $f$-functional unit to a difunctional one. For $f = 3$ and arbitrary $r$ we find (with $\alpha$ the fractional conversion of functionalities belonging to branch units):

$$\nu'_e = \frac{3}{2}[\alpha(1-\upsilon)]^3 = 12[1-(1/2r\alpha^2)]^3 \qquad (15)$$

since

$$\upsilon = [1 - r\alpha^2(2-\alpha)]/r\alpha^3 \qquad (16)$$

Assuming the density of the rubber is 1.0 g/cm$^3$, the number of EANCs per cm$^3$ is given, using $N$ for Avogadro's number, by:

$$\nu_e = 12[1-(1/2r\alpha^2)]^3\ \{2rN/[2 \times 269 \times r + 3 \times 11040]\} \qquad (17)$$

which leads to the following equation for the equilibrium shear modulus at 316K:

$$G_e/\mathrm{Nm}^{-2} = 1.873 \times 10^6 g[1-(1/2r\alpha^2)]^3 \qquad (18)$$

where $g$ is the front-factor, proposed to be unity above. Our *Figure 4* shows as the highest measured modulus, for $\alpha = r = 1$, $G_e = 1.92 \times 10^5$ Nm$^{-2}$ (corresponding to a front factor of $g = 0.82$).

For the case $f = 4$, we have

$$\upsilon = 1 - (3/2\alpha) + [(4r - 3r^2\alpha^2)^{1/2}/2r\alpha^2] \qquad (19)$$

and

$$\nu'_e = 2[\alpha(1-\upsilon)]^3[3 - 2\alpha(1-\upsilon)] \qquad (20)$$

and for density 1.0 g/cm$^3$, the theoretical modulus becomes, using equation (19):

$$G_e/\mathrm{Nm}^{-2} = 2.345 \times 10^5 g[\alpha(1-\upsilon)]^3[3 - 2\alpha(1-\upsilon)] \qquad (21)$$

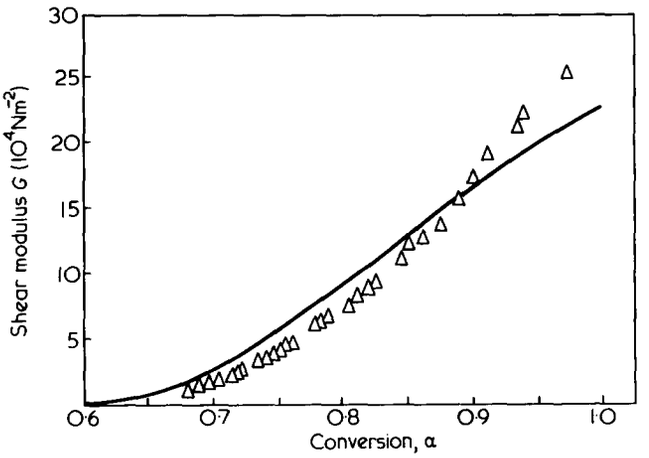


*Figure 6* Silicone[17] ($f = 4$, equation 12) data plotted as in *Figures 3* and *4*. Optimized fit to equation (21) (with equation 19), $r = 1$. For parameter $g$ see *Table 2*

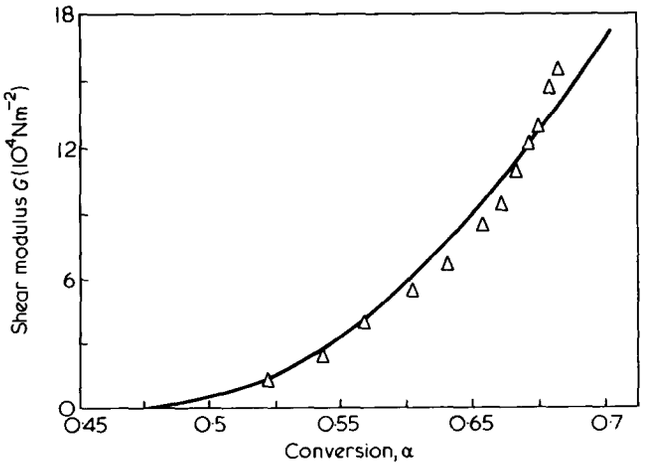


*Figure 7* Silicone data[17] for $f = 4$, $r = 1.56$ treated as in *Figure 6*

*Table 2* Front-factors $g$ obtained from Valles and Macosko's data by computer optimisation from equation 18 or 21 (with 19)

| Funtionality $f$ of branch units | Stoichiometric ratio $r$ | Figure and run | $g$ |
|---|---|---|---|
| 3 | 1 | 4: run A (triangles) (whole range) | 1.100 |
| 3 | 1 | 4: run B (squares) (whole range) | 0.982 |
| 3 | 1 | 5: run A (triangles) | 1.001 |
| 3 | 1 | 5: run B (squares) | 0.797 |
| 4 | 1.0 | 6 | 0.970 |
| 4 | 1.56 | 7 | 1.084 |
| | | Mean $g$ | 0.989 |
| | | (excluding squares) | 1.039 |

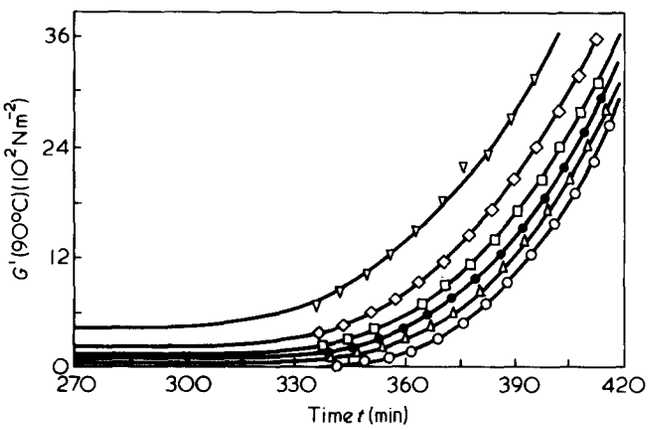


*Figure 8* Plots of $G'(\omega)$ against time for run 22 on stoichiometric DMG/BTA. Frequencies, from left to right: $\omega = 25$, $\omega = 10$, $\omega = 5$, $\omega = 2.5$, $\omega = 1.0$, $\omega = 0.1$ Hz. Optimized fits of equation (23) with (25), adjusting $t_c$, $G_f'(\omega)$, except that $G_f'(0.1)$ was constrained to be zero. Hence $g(0.1) \approx g(0) = 1.205$

The original *Figure 3* shows[17] an extrapolated value for $\alpha = 1$, $r = 1$: $G_e = 2.65 \times 10^5$ Nm$^{-2}$, which, compared with equation (21) implies a front factor $g = 1.13$. The least-square fit of equations (18) and (21) (with 19) gives front-factors of $g$ averaging 0.99 and deviating by no more than ±0.12 (see *Table 2*). The systematic deviations of the measurements from the fitted curves are similar in form to those found by Valles and Macosko[17] in fitting their entanglement theory, ours being slightly worse in *Figure 6*, and slightly better in *Figure 7*, than theirs. All three experimental runs do exhibit an increase, rather sharp in our *Figure 4*, in rate of increase in $G_e$ with conversion around $G_e \approx 1.2 \times 10^4$ Nm$^{-2}$, not modelled by our theory, nor that of Valles and Macosko. It seems likely that this effect reflects, not deviations from the models assumed for chemical kinetics or rubber elasticity, but possibly some instrumental error in measurements of moduli. *Figure 5* shows the result of excluding these suspect data, with modulus above $10^3$ N/m$^{-2}$, included in *Figure 4*. The data represented by squares seem to have suffered an error in the determination of the gel point.

Valles and Macosko's[17] original fits of these their data were based on the equations of Miller and Macosko, exemplified by the case $f = 3$, thus

$$\nu_e = \{4[1-(1/2r\alpha^2)]^3 + 16(\epsilon/\alpha^4)[1-(1/2r\alpha^2)]^4\}/[A_3]_0 \quad (22)$$

where $[A_3]_0$ is the concentration of branch units (mol m$^{-3}$).

The first term in the numerator on the right should be compared with the unique term on the right of equation (15), and is readily obtained from the quite general formalism of Dobson and Gordon[18] by weighting each active junction point by the factor (equation 7 above), equal in this case simply to a constant, viz. 1/3, suggested by Duiser and Staverman[1]. This substantial reduction in modulus, the theoretical justification of which is questioned above leads to *Figure 5B*. This reduction in modulus is compensated by the second term in equation (22), resting on the assumption of a contribution from entanglements.

## ANALYSIS OF NEW DYNAMIC DATA ON CRITICALLY BRANCHED DMG/BTA

Measurements of the real part of $G'(\omega)$ were performed in the range $0.1 \leqslant \omega \leqslant 25$ Hz on stoichiometric DMG/BTA mixtures at 90°C (controlled to ±0.05°C) in a suitably adapted Weissenberg Rheogoniometer (Farol Research Engineering Ltd). Data-handling was via a PDP 8 computer. Some experiments including benzene-*m*-diacetic acid were also found satisfactory but will be reported elsewhere. Data are fitted to theoretical curves for two runs in *Figures 8* and *9*, and parameters deduced from optimizing fits to the 10 best runs are given in *Table 3*. Each run consisted of a single kinetic experiment. Before gelation the viscosity was measured continuously at a constant shear rate not exceeding 85 sec$^{-1}$. After gelation, the real part $G'(\omega)$ of the shear modulus was charted by setting and resetting the frequency $\omega$ of the rheogoniometer to between 4 and 6 values sequentially (*Table 3*). The amplitude (0.03 rad) was small enough for applying the linear theory of viscoelasticity; $G'(\omega)$ was found constant over a forty-fold range of amplitudes.

Optimization of fits of the data-points to theory for $G'(\omega)$ *versus* time $t$ in *Figures 8* and *9* was in terms of two simultaneous equations. Equating the relative intermolecular conversion $\alpha/\alpha_c$ to $\beta/\beta_c$ (which includes the small intramolecular reaction component), and accordingly $\beta_c = 2^{-1/2}$, the first equation (cf. 18):

$$G'(\omega) = 12g(\omega)[A_3]_0 RT[1-(1/2\beta^2)]^3 + G_f'(\omega) \quad (23)$$

relates the storage modulus to conversion. The concentration $[A_3]_0$ of BTA units (mol m$^{-3}$) was based on the excel-

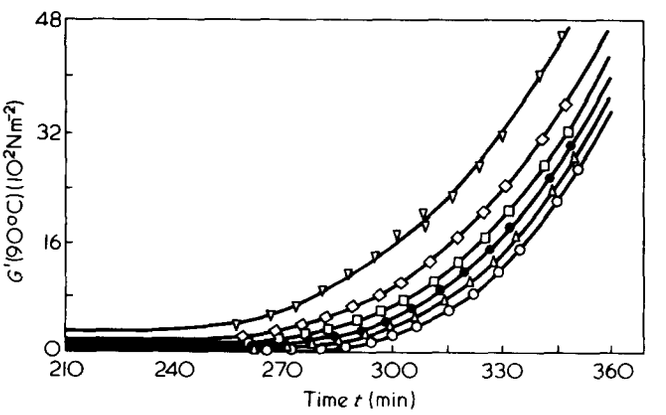


*Figure 9* As *Figure 8* but for replicate run 23. $g(0.1) \approx g(0) = 1.336$

*Table 3*
(a) Analysis of dynamic data on two typical runs (DMG/BTA, $r = 1$) at 90°C, using optimized fits to equation (23)

| Frequency (Hz) | Run | $t_{c,app}(\omega)$ | | $g(\omega)$ | | $G'_l$ Nm$^{-2}$ | | $\beta_{c,app}$ | | $\bar{M}_w \times 10^{-4}$ at $\beta_{c,app}$ | | Standard deviation $\sigma$ on $G'(\omega)$ (equation 23) ($10^2$Nm$^{-2}$) | |
|---|---|---|---|---|---|---|---|---|---|---|---|---|---|
| | | 21 | 23 | 21 | 23 | 21 | 23 | 21 | 23 | 21 | 23 | 21 | 23 |
| 25 | | 291.0 | 217.1 | 0.773 | 0.722 | 302 | 275 | 0.9941 | 0.9910 | 5.5 | 3.6 | 1.7 | 7.3 |
| 10 | | 302.9 | 233.6 | 0.802 | 0.831 | 264 | 155 | 0.9964 | 0.9942 | 8.9 | 5.6 | 1.8 | 1.3 |
| 5 | | 309.7 | 244.4 | 0.848 | 0.954 | 176 | 111 | 0.9976 | 0.9963 | 13.9 | 8.8 | 0.6 | 1.4 |
| 2.5 | | 314.2 | 251.4 | 0.889 | 1.053 | 113 | 75 | 0.9985 | 0.9976 | 21.7 | 13.7 | 0.8 | 1.3 |
| 1 | | 318.7 | 257.6 | 0.953 | 1.173 | 62 | 42 | 0.9993 | 0.9988 | 49.3 | 26.9 | 0.7 | 1.1 |
| 0.1 | | 322.3 | 264.1 | 0.995 | 1.336 | 0 | 0 | 1.0000 | 1.0000 | ∞ | ∞ | 0.9 | 1.1 |

(b) Front-factors $g(0.1)$ for ten best runs

| Run | 13 | 20 | 21 | 22 | 23 | 24 | 25 | 27 | 28 | 29 | Mean | $\sigma$ |
|---|---|---|---|---|---|---|---|---|---|---|---|---|
| $g(0.1)$ | 1.190 | 0.895 | 0.995 | 1.205 | 1.336 | 1.125 | 0.928 | 0.916 | 0.815 | 1.004 | 1.041 | 0.157 |

(c) Mean front-factors $g(\omega)$

| Number of runs available | 5 | 10 | 10 | 5 | 10 | 10 |
|---|---|---|---|---|---|---|
| frequency $\omega$(Hz) | 25 | 10 | 5 | 2.5 | 1.0 | 0.1 |
| $\langle g(\omega) \rangle$ | 0.644 | 0.695 | 0.764 | 0.895 | 0.915 | 1.041 |
| $\sigma$ for $\langle g(\omega) \rangle$ | 0.121 | 0.131 | 0.109 | 0.117 | 0.146 | 0.166 |

lent approximation of specific gravity equal to 1.0 g/cm$^3$ and the formula (see equation 17):

$$[A_3]_0 = 2/[3 \times 174.29 + 2 \times 252.23 - 6\beta \times 18.02] \quad (24)$$

The first term on the right of equation (23) follows from equation (15) for the ring-free model (for $r = 1$, $\alpha = \beta$) and is constrained to be zero before the gel point. The second term $G'_l(\omega)$ makes allowance for a constant finite liquid-type contribution, at any given frequency, to the modulus from non-EANC sources both before and after gelation.

The second equation in the optimization serves to determine $\beta$ as a function of measured time, $t$, for insertion into equation (23). This is the third-order kinetic law (see *Figure 2*):

$$(1-\beta)^{-2} - (1 - 2^{-1/2})^{-2} = 2k(t - t_c) \quad (25)$$

with $k = 5.24 \times 10^{-3}$ min$^{-1}$ as determined (*Table 1*) by independent titration measurements. The optimization was based on the assumption that the lowest frequency used, $\omega = 0.1$ Hz, would be close enough to zero for the fitting of this bottom curve (*Figure 8* and *9*) to be optimized over the two parameters $t_c$ and $g(\omega)$ only, while setting $G'_l(0.1) = 0$. It is seen that this does represent the data, and the curves at $\omega = 0.1$ are shown below to be close to the theoretical limit $G'(0)$ by an empirical extrapolation (equation 27). At the higher frequencies, $G'_l(\omega)$ was a third parameter for optimization, and though its contribution is small, it renders the optimized parameter values less accurate.

The apparently critical conversion $\beta_{c,app}(\omega)$ falls with increasing frequency, as the apparent gel point $t_{c,app}(\omega)$ occurs progressively earlier (*Figure 8* and *9*). This $\beta_{c,app}$ is set equal to $\beta_c = 2^{-1/2}$ at the minimal frequency of 0.1 sec$^{-1}$, and calculated (*Table 2*) from the equation (see 25):

$$[1 - \beta_{c,app}(\omega)]^{-2} - (1 - 2^{-1/2})^{-2} = 2k[t_{c,app}(\omega) - t_c(0.1)] \quad (26)$$

for other frequencies. The fitting procedure thus defined amounts to absorbing the disturbing effect of frequency on $G'(\omega)$ by the same rescaling procedure, based on the critical (gel) point, as applied to the small incursion of intramolecular bonding, in accordance with the established methodology in the field of critical phenomena (see, e.g. Fisher and Scesney[19]). The important parameter for our purpose is $g(\omega)$. In every run, the value of $g(\omega)$, found by optimizing, rose as frequency decreased from 25 to 0.1 Hz. The mean $g(25)$ over the five available runs was 0.644 (*Table 3c*).

The plots of $G'(\omega)$ vs. $t/t_c$ should, of course, converge to a single curve at high enough conversion when the rubber has become perfectly elastic, as shown for their silicone rubbers by Valles and Macosko[17] in their *Figure 1* over a $10^5$-fold frequency range. The convergence is just perceptible in our *Figures 8* and *9* at the high modulus end.

Even for the quasi-static measurements of 0.1 Hz, two parameters, $t_c$ and $g(0.1)$ are adjusted in the optimization according to equation (23). However, since the optimized parameters agree well with values available independently, the fit can be described as practically parameter-less.

(i) First we compare $t_c$ obtained by optimization according to equation (23), representing back-extrapolation of the modulus, with $t_c$ obtained from forward extrapolation of the viscosity (see *Figure 3*) in the same run. Equivalently, we may translate the $t_c$ values to $\beta_c$ values (equation 25). It emerges that $\beta_c$ from back-extrapolation of the modulus is generally between 0.002 and 0.005 lower than the value from viscosity. This *small* discrepancy is significant and intelligible, because shear-rate effects will raise the viscometric gel point, but lower (*Table 3a*) the gel point from modulus data.

(ii) Secondly, the front-factor $g$, equated to $g(0.1)$, agrees within the documented experimental error with the classical value of unity, rehabilitated by theoretical arguments in the Theory section above (*Table 3*). To show this, we have calculated the $g$-values from optimization of the 10 trustworthy replicate runs in *Table 3b*, which range from 0.815 up to 1.336 (*Figure 9*), with mean value 1.041 and standard deviation 0.157. Dividing this standard deviation by the square root of the number 9 of degrees of freedom for 10 data points, gives 0.052 as the standard deviation of the mean front-factor. The mean 1.041 itself compares satisfactorily with the value 0.920 obtained by taking into account, not merely the $g(0.1)$ values, but the whole range of data. Thus the 50 curves available for 6 frequencies, mostly with over 10 data points each, yielded the mean front factors $\langle g(\omega)\rangle$ listed in *Table 3c*. These were fitted to the empirical extrapolation formula:

$$g(\omega) = 0.920 \exp(-0.0168\,\omega) \qquad (27)$$

with coefficient of determination $r^2 = 0.74$, which gives $g(0) = 0.920$. The exponent $-0.0168$ cannot be trusted quantitatively, but the decline of $g(\omega)$ with increasing $\omega$ is clearly real and indeed expected. It represents delay in the rate of build-up of the effective network due to orientational effects on the chains under shear.

## DISCUSSION

Valles and Macosko[16] open their paper with the statement: 'The statistical theory of rubber elasticity is one of the simplest and most successful theories in polymer science.' Our work not only confirms this verdict but simplifies the theory back to its much earlier form, by reinstating the classical front-factor $g = 1$ and by eliminating the parameter $\epsilon$ and the contribution from entanglements which it aims to model. These simplifications leave the fit to their own data, and ours on a complementary network-forming system, within experimental error, essentially without adjustment of parameters. In fairness, it should be pointed out that the value $\epsilon = 62$ mol m$^{-3}$ used by these authors agrees well with deduction by Langley and Ferry[20] from dynamics of linear poly(dimethyl siloxane), and by Langley and Polmanteer[21] for the radiation crosslinked polymer. On the other hand, our new measurements on DMG/BTA suggest that the effect of entanglements is at least greatly exaggerated by the value of $\epsilon$ just cited, for the following reason. Our measurements were deliberately taken in the range of critically-branched structures near the gel point, recommended for eliminating disturbances from rubber elasticity studies by Dobson and Gordon[18]. We calculate that the mean value of the term in equation 22 for our range of conversion $\alpha$ to be 1/13 that for their higher range of conversion on the silicone system, thus essentially eliminating the effect of entanglements (see *Figure 5*). Yet both systems are here fitted to values of $g$ close to unity (which we back theoretically), while $\epsilon = 62$ requires $g \approx 1/3$.

In assessing the reliability of the kinetic calibration of conversion we recall our warning that the percentage error in the rate constant is tripled when passing to $g$. It may be thought that there is evidence in *Figure 2* that the apparent rate constant of the linking process in DMG/BTA increases just before the gel point, where points lie above the calibration line. If so, the front factor would be lowered. Independent measurements by the steam pressure technique on similar esterification reactions[5] have, however, shown that the rate behaviour is quite regular through the gel point region, without any increase in apparent rate constant. In particular, the apparent rise in the last three titrations in *Figure 2* is certainly much larger than that accountable for by the neglect of the small cyclization component, as confirmed by computer calculation. Titration of nearly gelled materials is hazardous, and we believe the calibration line to reflect the correct rate constant to about 1% accuracy (*Table 1*) throughout the critical branching region used for our dynamic measurements.

The value $g = 1$, strongly supported by measurements on the same system DMG/BTA using the microsphere-rheometer[5], is now confirmed by the more accurate computerized cone-and-plate instrument.

### *Role of entanglement theory*

The entanglement notion serves as a correction to polymer theories, which makes sense when matter, represented by chain-graphs, is embedded in a three-dimensional space. The notion of a *physical space* is extremely helpful in the postulation and construction of physical theories. Since Kant's 'Critique of Pure Reason' most physicists have gone further and taken its 'existence' to be proven, though Leibniz would have frowned at such ontological commitment. Flory's notion of a *phantom chain* invites us not to take seriously the embedding space of a rubber. It turns out that many physical properties of amorphous systems are well modelled by unembedded molecular graphs. This has been illustrated in earlier parts of this series of papers entitled the 'Graph-like state of matter' (see refs 7 and 22). Using the present experimental data, and their analysis we consider first equilibrium and then dynamic entanglement theories from this viewpoint.

### *Equilibrium modulus and permanent entanglements*

The experimental values of the front-factor $g$, collected with averages and standard deviations in *Tables 2* and *3c*, demonstrate that present experiments on two diverse network-forming systems are far from accurate enough to detect deviations from the purely graph-like classical model ($g = 1$). In other words, rubber elasticity here provides no evidence of effects involving an embedding space, or that the physical world is three-dimensional. Effects which have been derived from theory, some increasing and some decreasing the modulus, have thus cancelled out, if indeed the theories are to be trusted.

The various approaches to the factors leading to supposed *reductions* in $g$ (for the usual case $f = 4$) are hard to review. They do not merely treat the same aspects of the basic model. Eichinger's[23] argument for $g = \frac{1}{2}$ is purely graph–theoretical and does not involve the embedding space. James and Guth[4] based their estimate of $g = \frac{1}{2}$ on a supposed statistical effect, which is no longer accepted, leading to a shrinkage of the network in the course of its formation. Edwards[24] obtained the same estimate from self-consistent field calculations; Imai and Gordon[3] from considering the correlations in Brownian motion between neighbouring network chains attached to the same active junction. It is perhaps not always certain that calculated second-order effects are not nullified by the large number of neglected terms, which are taken to be individually of higher order.

The *increase* in $g$ derived from the notion of entanglements could easily be overestimated. Sound statistical cal-

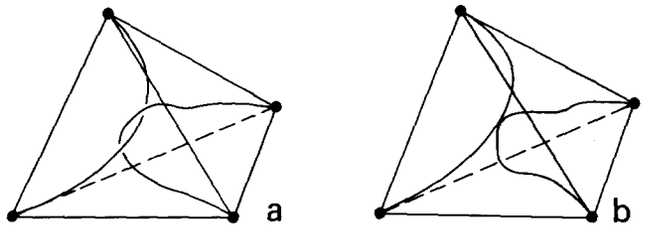


*Figure 10* (a) Permenent entanglement after Ziabicki[25]; (b) neighbouring configuration which has just escaped entanglement during vulcanization

culations by Ziabicki[25], containing the necessary integrations over configuration space, are based on the self-explanatory model of *Figure 10a*. He has emphasized the caution required in applying the estimates obtained to the whole molecular network of a real rubber. There is an immediate way of visualizing the difficulty. The desired effect due to an entanglement depends on the change during deformation in the ratio of the number of allowed configurations for phantom chains (passing freely through each other), to that forbidden to real chains entangled as in *Figure 10a*. The trouble is that during crosslinking the two chains are almost equally likely just to escape becoming entangled, viz. by becoming fixed in configuration *10b*. This configuration allows the states forbidden to *Figure 10a*, and *vice versa*. If *Figure 10a* leads to greater restriction on freedom during deformation (which depends, as Ziabicki has noted, on the direction of the strain), then *10b* becomes correspondingly less restricted. The net effect on the modulus, to be caught in the front-factor, must therefore be small. Edwards[26] has shown that the net effect is positive, in the direction of increasing $g$. Langley[27] regards the entanglement parameter $\epsilon$ in equation (22) as (one half of) the 'maximum potential contribution of entanglements' to the modulus, which 'should be regarded as the product of the potential entanglement density and the effectiveness of a trapped entanglement relative to a chemical crosslink'. He does propose a plot which in principle could determine $\epsilon$ from dynamic measurements. We believe, however, that theory as well as experiments need refinement to establish the actual net effect of entanglements on the modulus at equilibrium, which is likely to be too small to concern technology.

*Dynamic entanglements*

The entanglement concept is of incomparably greater utility in treating dynamic effects than in equilibrium theories. We shall sketch in qualitative terms how our new measurements are rationalized in terms of this concept, but also how a quantitative theory is likely to be ultimately simpler if the mathematical model is freed from postulates which depend on the topology of an embedding space.

The frequency shifts observed over 250-fold range of frequency in typical *Figures 8* and *9* are characteristic of the critical-branching region near the gel point. At higher conversions, these curves would converge to a single one, a process just noticeable at the high-modulus end. The silicone rubbers of Valles and Macosko[17], featuring much higher degrees of crosslinking and moduli, had reached the asymptotic state of perfectly elastic bodies (their *Figure 1*) over a wider frequency range. Current theory attributes the anelastic effects revealed by frequency shifts to a conversion, which rises with increasing frequency, of relaxable entanglements into active junction points, which contribute unrelaxed physical crosslinks in addition to chemical crosslinks (covalencies). This leads, as it should, to the apparent gel point being observed earlier. The narrow range of states between this apparent gel point and the true one begins to make manifest a continuous region of states intermediate between a true gel point and a true entanglement transition. The true entanglement transition is, of course, well documented in linear polymer systems[28], where it is reflected in a sudden increase of the viscosity exponent when the weight-average molecular weight $\bar{M}_w$ passes through some value in the range $10^4$–$10^5$. At our highest frequency of 25 Hz, available from 5 separate runs with DMG/BTA which may be compared with individual results for two runs at the end of *Table 3a*, we calculate the following results. The apparent critical conversion was 0.992 with standard deviation 0.003. $\bar{M}_w$ at this conversion was $4.7 \times 10^4$ with standard deviation $1.7 \times 10^4$. It is plausible that the apparent critical conversion is approaching some limit as the frequency is increased, and that $\bar{M}_w$ thus approaches a value typical for the entanglement transition of linear systems.

The notion of entanglement is, of course, inspired by our intuitive insight into the topological structure of a three-dimensional space. Yet the signs are that even dynamic properties, so plausibly explained in qualitative and even quantitative terms, will ultimately be modelled by purely one-dimensional theories based on graphs unembedded in a Riemannian space, thus simplifying the conceptual framework and the mathematics. Occam's razor was applied in this way to the Rouse model, which is fundamental for chain dynamics, when Forsman[29] reduced the calculations of Rouse spectra to an eigenvalue problem belonging to unembedded graphs. Chompff and Duiser[30] obtained the spectrum of a whole regular chain network by appropriate summation of the different spectra of suitably decoupled (non-overlapping) chain-segments. They also explicitly extended their treatment to 'entanglement-networks', essentially by introducing fractional weights to points of unembedded graphs. Such points represent notionally those contacts which are weaker than covalent crosslinks in an unembedded model. The present measurements on DMG/BTA suggest that, as is usual, the solution for a completely random system will finally be simpler than for regular networks; but, as is also usual, this will require some novel combinatorial analysis. The following intriguing observations offer a starting point.

*Figure 11* shows typical plots of $G'(\omega)$ against $\omega$ over the 250-fold frequency range available in this work for different degrees $\alpha/\alpha_c$ of relative conversion in the critical region. The plots become more concave, viewed from the frequency axis, as $\alpha/\alpha_c$ increases. For a liquid before gelation

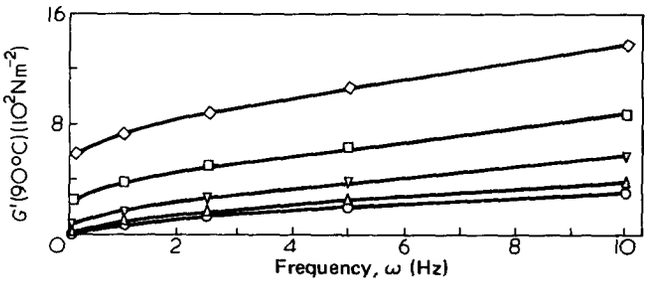


*Figure 11* Typical plot of $G'(\omega)$ against frequency $\omega$ at different conversions in run 21. Relative conversions $\beta/\beta_c$ are: ◇, 1.0100; □, 1.0075; △, 1.0050; △, 1.0025; ○, 1.0000 (= gel point). Note that at the gel point the plot is almost linear, but appreciable curvature has developed at $\beta/\beta_c = 1.01$

($\alpha/\alpha_c < 1$), some positive contribution to $G'$ at high $\omega$, and a convex-downward course, would be expected. (Only weak evidence was found for this expected behaviour of viscoelastic pre-gel DMG/BTA because of instrumental difficulties.) However, the rapid approach to the linear equation:

$$G'(\omega) = k\omega \tag{28}$$

with $k$ a constant, as $\alpha/\alpha_c \downarrow 1$ (gel point) over the narrow range $1.01 \leqslant \alpha/\alpha_c \leqslant 1.00$, is striking. This suggests that equation (28) represents a new, presumably quite general law for the sharp characterization of a gel point. If this equation remains valid at the gel point over a sufficient range of frequencies, the corresponding spectrum of relaxation frequencies, $\bar{N}(\omega)$, is readily calculated from the standard theory of linear viscoelasticity[31], viz. a block distribution:

$$\bar{N}(\omega) = k/\pi \tag{29}$$

Accordingly, every positive relaxation frequency is equally probable at the gel point.

Now it has been shown that gels of DMG/BTA have practically a tree-like structure (few cycles)[15]. Statistical theory demonstrates that if we define a chain-segment in a tree-like gel at $\alpha/\alpha_c = 1$ as a chain lying between any two branch-points in a molecule of the system (i.e. including the whole of the soluble fraction with the infinitesimal weight-fraction of gel), then the length-distribution of all chain-segments is precisely a block distribution. The chain-segments so defined overlap copiously, so that a given chemical bond may belong to many such chain-segments, which renders a straightforward decoupling procedure inapplicable. Accordingly, the solution of the eigenvalue problem of the Rouse matrix of a random, critically branched, system at the gel point remains an open problem requiring urgent solution.

## HISTORICAL PERSPECTIVES

The historical review by Dušek and Prins[32] on the structures and elasticity of networks was the first to give adequate weight to the detailed statistical structure of the underlying molecular graphs, based on the notion of an active chain put forward by Scanlan[33] and by Case[34]. More recently, Graessley[2] remarked that 'conflicts regarding $g$ are annoying, not only because they concern the foundations of an otherwise attractive and successful molecular theory, but also because they prevent an unequivocal separation of chemical network contributions from other contributions such as chain entanglement, to the observed properties of real networks'. This remark, with its reminder of the role that experiment has to play, is equally valid for the other constants in the equation of state of a rubber. Mark and coworkers have made especially valuable studies[35], refining measurements so that controversies regarding the multiplying constant of the logarithmic swelling term and the constant $C_2$ might be settled. The characterization of the model networks plays an important part in refining measurements. The system DMG/BTA, prepared in the melt from pure, crystalline monomers, has previously been characterized by light-scattering[15], sol fraction studies[15], equilibrium[36] and sedimentation velocity[37] ultracentrifuge methods, gel chromatography[38], and other techniques, and was the subject of favourable comment from Flory[39]. The present study set out to exploit the peculiarity of the region of critical branching around the gel point, which allows disturbances such as contributions from entanglements and cycles to be minimized[18,40]. In fact, the exploitation of critical phenomena, together with the appropriate rescaling procedures, are too widely diffused and successful in chemical physics to need further commendation. Perhaps the advantages of the strategy are purchased at the expense of more sophisticated control and measuring equipment, e.g. here to deal with highly viscous liquids or weak gels. Buch such equipment is now readily available.

It would be too sanguine to hope that our theoretical arguments in the Front-Factor Theory will finally settle 'the conflicts regarding $g$'. The drive to pare down models requiring multidimensional continua to the combinatorial structure of graphs involves no deep or metaphysical principles. Usually the aim is to reinterpret in simpler formal mathematics those operations which reflect the properties of supposedly continuum-based models, which have actually been used (as distinct from merely postulated at the outset) in more classical deductions. Those interested in extending such efforts for recasting theories of networks, as well as the general reader, will find Graessley's review[41] of the entanglement concept quite invaluable.

## ACKNOWLEDGEMENT

We thank Mr B. W. Ready for extensive help with the computerization of control of, and handling data from, the rheogoniometer.

## REFERENCES

1 Duiser, J. A. and Staverman, A. J. 'Physics of Non-Crystalline Solids', (Ed. J. A. Prins) North Holland, Amsterdam, 1965, p 376
2 Graessley, W. W. *Macromolecules* 1975, **8**, 186
3 Imai, S. and Gordon, M. *J. Chem. Phys.* 1969, **50**, 3889
4 James, H. M. and Guth, E. *J. Chem. Phys.* 1947, **15**, 669
5 Gordon, M., Ward, T. C. and Whitney, R. S. 'Polymer Networks' (Eds. A. J. Chomff and S. Newman) Plenum Press, New York and London, Vol 1, 1970
6 Gordon, M. and Ross-Murphy, S. B. *Pure Appl. Chem.* 1975, **43**, 1
7 Dušek, K., Gordon, M. and Ross-Murphy, S. B. *Macromolecules* 1978, **11**, 236
8 Wall, F. T. and Flory, P. J. *J. Chem. Phys.* 1951, **19**, 1435
9 Stepto, R. F. T. and Waywell, D. R. *Makromol. Chem.* 1972, **152**, 263
10 Hinshelwood, C. N. and Legard, A. R. *J. Chem. Soc.* 1935, p 587
11 Flory, P. J. *J. Am. Chem. Soc.* 1939, **61**, 3334
12 Gordon, M. and Leonis, C. G. *J. Chem. Soc. (Faraday Trans. I)* 1974, **71**, pp 161, 178
13 Gordon, M. and Scantlebury, G. R. *J. Chem. Soc.* 1967, p 1
14 Gordon, M. and Scantlebury, G. R. *Proc. Roy. Soc. (A)* 1966, **292**, 380
15 Peniche-Covas, C., Dev, S. B., Gordon, M., Judd, M. and Kajiwara, K. *Discuss. Faraday Div.* 1974, **57**, 165
16 de Gennes, P. -G. in press
17 Valles, E. M. and Macosko, C. W. 'Chemistry and Properties of Crosslinked Polymers', (Ed. S. S. Labana) Academic Press, New York, 1977
18 Dobson, G. R. and Gordon, M. *J. Chem. Phys.* 1965, **43**, 705 and *Rubber Chem. Technol.* 1966, **39**, 1472
19 Fisher, M. E. and Scesney, P. E. *Phys. Rev. (A)* 1970, **2**, 825
20 Langley, N. R. and Ferry, J. D. *Macromolecules* 1968, **1**, 353
21 Langley, N. R. and Polmanteer, K. E. *J. Polym. Sci. (Polym. Phys. Edn)* 1974, **12**, 1023
22 See ref 7 and: Gordon, M., Torkington, J. A. and Ross-Murphy, S. B. *Macromolecules* 1977, **10**, 1090; Gordon, M. and Ross-Murphy, S. B. *J. Phys. (A)* 1978, **11**, L155
23 Eichinger, B. E. *Macromolecules* 1972, **5**, 496

24 Edwards, S. F. in 'Polymer Networks', (Eds. A. J. Chompff and S. Newman) Plenum Press, New York, 1971
25 Ziabicki, A. *J. Chem. Phys.* 1976, **64**, 4100, 4107
26 Edwards, S. F. in personal conversation
27 Langley, N. R. *Macromolecules* 1968, **1**, 348
28 Ferry, J. D. 'Viscoelastic Properties of Polymers', 2nd Edn. Wiley, New York, 1970
29 Forsman, W. C. *J. Chem. Phys.* 1976, **65**, 4111
30 Chompff, A. J. and Duiser, J. A. *J. Chem. Phys.* 1966, **45**, p 1505
31 Gross, B. 'Mathematical Structure of the Theories of Viscoelasticity', Hermann & Cie., Paris, 1953
32 Dušek, K. and Prins, W. *Adv. Polym. Sci.* 1969, **6**, 1
33 Scanlan, J. *J. Polym. Sci.* 1960, **43**, 501
34 Case, L. C. *J. Polym. Sci.* 1960, **45**, 397
35 Mark, J. E. and Johnson, R. M. *Macromolecules* 1972, **5**, 41; Mark, J. E. and Yu, C. U. *Ibid.* 1973, **6**, 751
36 Gordon, M., Leonis, C. G. and Suzuki, H. *Proc. Roy. Soc. London (A)* 1975, **346**, 207; *Makromol. Chem.* 1977, **178**, 1867
37 Suzuki, H. and Leonis, C. G. *Br. Polym. J.* 1973, **5**, 485
38 Clarke, N. S., Devoy, C. J. and Gordon, M. *Br. Polym. J.* 1971, **3**, 194
39 Flory, P. J. *Discuss. Faraday Div.* on Gels and Gelling Processes, **57**, opening lecture
40 Gordon, M. *Trudy Mezhdinarodnoi Conferencii po Kautshuku i Resine, Chimia, Moscow*, 1971
41 Graessley, W. W. *Adv. Polym. Sci.* 1974, **16**, 1